

## Supporting Information

### Unraveling the Single Atomic Active Site under

### Realistic Simulated Natural Heme-containing Enzymes

Chao Zhao,<sup>‡a</sup> Can Xiong,<sup>‡a</sup> Xiaokang Liu,<sup>‡c</sup> Man Qiao,<sup>d</sup> Zhijun Li,<sup>a</sup> Tongwei Yuan,<sup>e</sup> Jing Wang,<sup>a</sup> Yunteng Qu,<sup>a</sup> XiaoQian Wang,<sup>a</sup> Fangyao Zhou,<sup>a</sup> Qian Xu,<sup>c</sup> Shiqi Wang,<sup>a</sup> Min Chen,<sup>a</sup> Wenyu Wang,<sup>a</sup> Yafei Li,<sup>d</sup> Tao Yao,<sup>c</sup> Yuen Wu,<sup>\*a</sup> and Yadong Li<sup>b</sup>

*<sup>a</sup>School of Chemistry and Materials Science, Hefei National Laboratory for Physical Sciences at the Microscale, University of Science and Technology of China, Hefei 230026, China.*

*<sup>b</sup>Department of Chemistry, Tsinghua University, Beijing 100084, China.*

*<sup>c</sup>National Synchrotron Radiation Laboratory, University of Science and Technology of China, Hefei, 230029, China.*

*<sup>d</sup>Jiangsu Collaborative Innovation Centre of Biomedical Functional Materials, School of Chemistry and Materials Science, Nanjing Normal University, Nanjing 210023, China.*

*<sup>e</sup>NEST Lab, Department of Chemistry, College of Science, Shanghai University, Shanghai 200444, China.*

## **Table of contents**

**1. Material Synthesis and Characterization**

**2. Catalytic Measurements**

**3. Supporting Figures and Tables**

# 1. Material Synthesis and Characterization:

## Chemicals.

Analytical grade Zinc nitrate hexahydrate ( $\text{Zn}(\text{NO}_3)_2 \cdot 6\text{H}_2\text{O}$ ), 2-methylimidazole were obtained from Shanghai Chemical Reagents, China. iron powder were purchased from Alfa Aesar. All of the chemicals used in this experiment were analytical grade and used without further purification.

## Methods

### Experimental Section.

#### Synthesis of ZIF-8.

In a normal procedure,  $\text{Zn}(\text{NO}_3)_2 \cdot 6\text{H}_2\text{O}$  (0.546 g) and 2-methylimidazole (0.616 g) were dissolved in 15 mL of methanol, respectively. Then the  $\text{Zn}(\text{NO}_3)_2 \cdot 6\text{H}_2\text{O}$  in methanol solution was rapidly injected into solution of 2-methylimidazole under ultrasound for 10 min at room temperature. The resulting suspension was transferred to 50 mL Teflon-lined stainless-steel autoclaves and then heated at 393 K for 4 h. Finally, the as-obtained precipitates were centrifuged and washed with methanol several times and dried in vacuum at 343 K for overnight.

#### Synthesis of Fe SAEs.

The powder of ZIF-8 and Fe powder were placed on either side of the boat and then heated to the desired temperature (1200 °C) for 6 h at the heating rate of 5 °C/min under flowing  $\text{N}_2$  gas and then naturally cooled to room temperature to obtain the representative samples. The as-prepared products were directly used without any post-treatment.

## Characterizations.

Powder X-ray diffraction patterns of samples were recorded using a Rigaku Miniflex-600 with  $\text{Cu K}\alpha$  radiation ( $\text{Cu K}\alpha$ ,  $\lambda=0.15406$  nm, 40 kV and 15 mA). The morphologies are characterized by TEM (Hitachi-7700, 100KV). The high-resolution TEM, HAADF-STEM images the corresponding Energy dispersive x-ray spectroscopy were recorded by a FEI Tecnai G2 F20 S-Twin high-resolution transmission electron microscope working at 200 kV and on a JEOL JEM-ARM200F TEM/STEM with a spherical aberration corrector working at 300 kV. The SEM was carried out by a JSM-6700F SEM. Nitrogen sorption measurement was conducted using a Micromeritics ASAP 2020 system at 77 K. Photoemission spectroscopy experiments (XPS) were performed at the Catalysis and Surface Science End station at the BL11U beam line of National Synchrotron Radiation Laboratory (NSRL) in Hefei, China. Elemental analysis of Fe in the solid samples was detected by an Optima 7300 DV inductively coupled plasma atomic emission spectrometer (ICP-AES). XAFS measurement and data analysis: XAFS spectra at the Fe K-edge were recorded at the 1W1B station of the Beijing Synchrotron Radiation Facility (BSRF), China. The Fe K-edge XANES data were recorded in a fluorescence mode. Fe foil and  $\text{Fe}_2\text{O}_3$  were used as references. The storage ring was working at the energy of 2.5 GeV. The hard X-ray was

monochromatized with Si (111) double-crystals. The acquired EXAFS data were extracted and processed according to the standard procedures using the ATHENA module implemented in the IFEFFIT software packages. The  $k^3$ -weighted EXAFS spectra were obtained by subtracting the post-edge background from the overall absorption and then normalizing with respect to the edge-jump step. Subsequently,  $k^3$ -weighted  $\chi(k)$  data in the  $k$ -space ranging from 2.5–11.2  $\text{\AA}^{-1}$  were Fourier transformed to real (R) space using a hanning windows ( $dK = 1.0 \text{\AA}^{-1}$ ) to separate the EXAFS contributions from different coordination shells.

## 2. Catalytic Measurements.

The steady-state kinetic assays were monitored in times can mode at 652 nm for TMB and 427 nm for OPD using a THERMO Varioskan Flash spectrophotometer. Catalytic experiments were carried out as follows: 5  $\mu\text{g/mL}$  Fe SAEs (final concentration) in HAC-NaAc buffer solution (pH=3.8) treated with 100  $\mu\text{L}$  of TMB/OPD (0.1-2 mM) as a substrate and 100  $\mu\text{L}$  of  $\text{H}_2\text{O}_2$  (6 mM), or 100  $\mu\text{L}$  of  $\text{H}_2\text{O}_2$  (0.06-6 mM) as a substrate and TMB/OPD (2 mM) with a total reaction volume of 200  $\mu\text{L}$  at 37  $^\circ\text{C}$ . The apparent kinetic parameters were calculated based on the function  $v = (V_{\text{max}} \times [S]) / (K_m + [S])$ , where  $v$  is the initial velocity,  $V_{\text{max}}$  is the maximal reaction velocity,  $[S]$  is the concentration of substrate and  $K_m$  is the Michaelis constant.

Calculate the specific activity of the Fe SAEs (U/mg) using the following equation:  $a = V / (\varepsilon \times l) \times (\Delta A / \Delta t)$ , where  $a$  is the specific activity expressed in units per milligram (U/mg);  $V$  is the total volume of reaction solution ( $\mu\text{L}$ );  $\varepsilon$  is the molar absorption coefficient of the colorimetric substrate;  $l$  is the path length of light travelling in the cuvette (cm);  $A$  is the absorbance after subtraction of the blank value; and  $\Delta A / \Delta t$  is the initial rate of change in absorbance.

### Electron paramagnetic resonance (EPR) experiments.

EPR measurements were performed using the JES-FA200 system. 5, 5-dimethyl-1-pyrroline N-oxide (DMPO) (98%, Alfa Aesar) was selected as the spin trapping agent to capture active species in the reaction. The same quartz capillary tube was used to minimize experimental errors in all EPR measurements. In a normal measurement, 5  $\mu\text{g/mL}$  Fe SAEs was added to a mixture of 100  $\mu\text{L}$  TMB, 100  $\mu\text{L}$   $\text{H}_2\text{O}_2$  and 50  $\mu\text{L}$  DMPO in 1 mL HAC-NaAc buffer solution (pH 3.8). EPR spectrum was recorded after 1 min of reaction.

### 3. Supporting Figures and Tables.

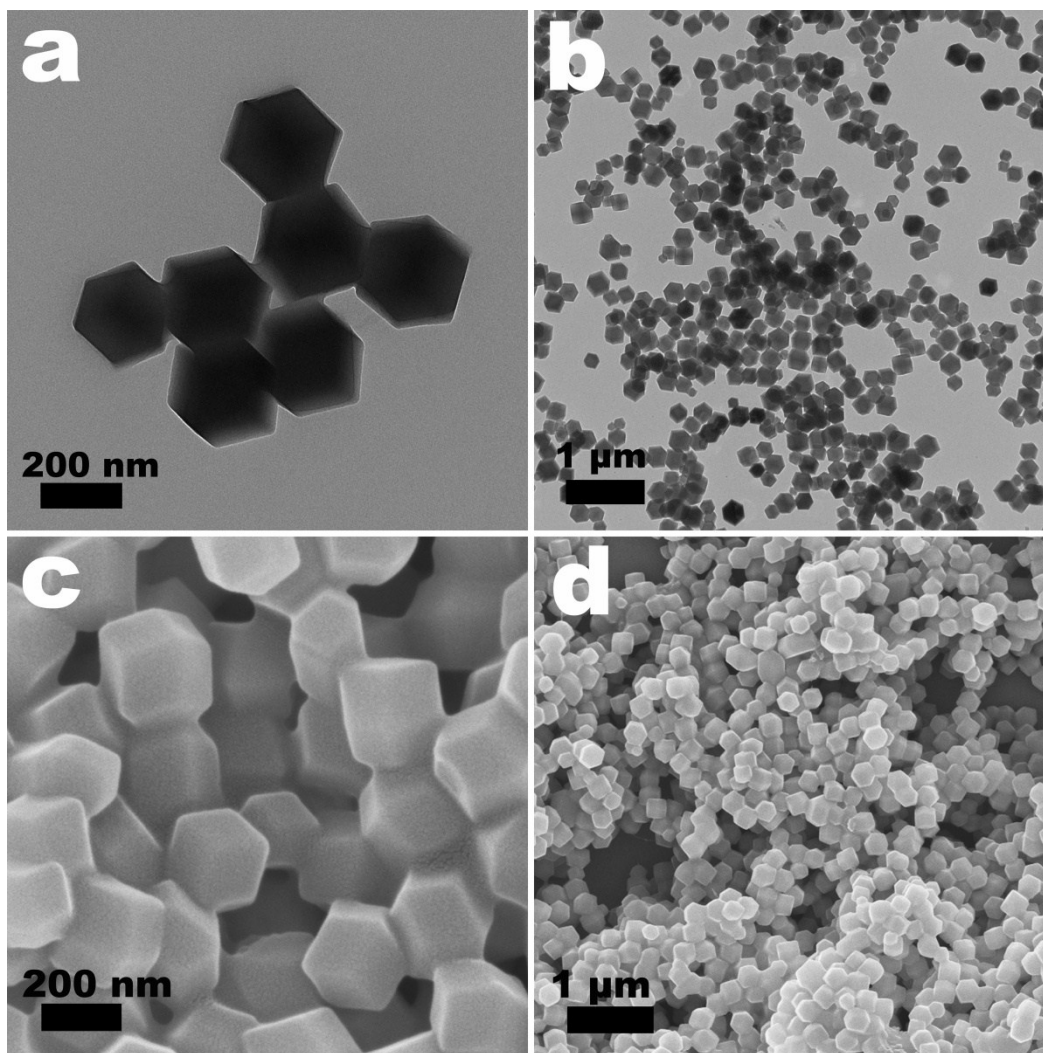


**Figure S1.** TEM image and SEM image of ZIF-8.

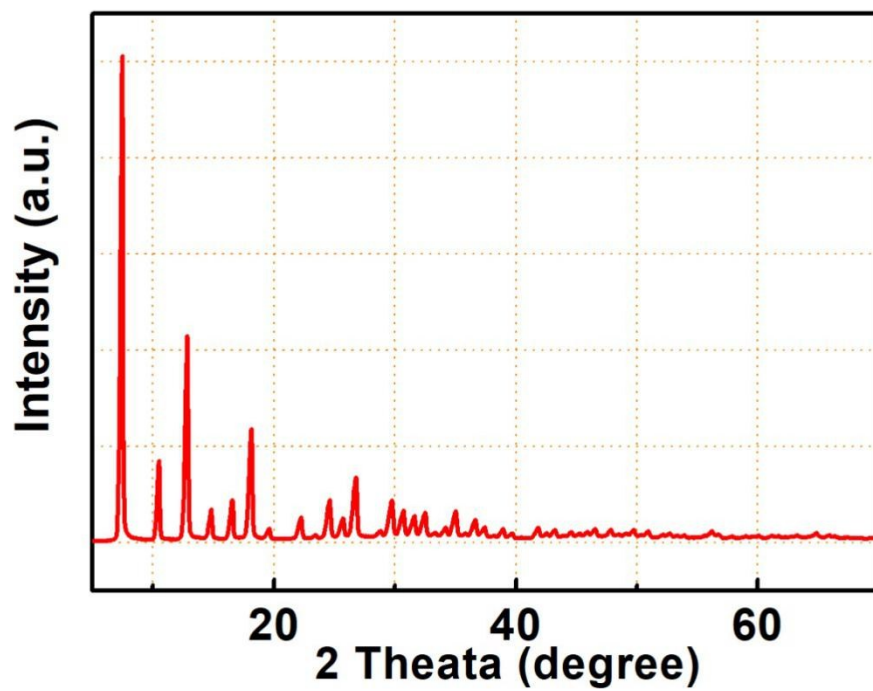
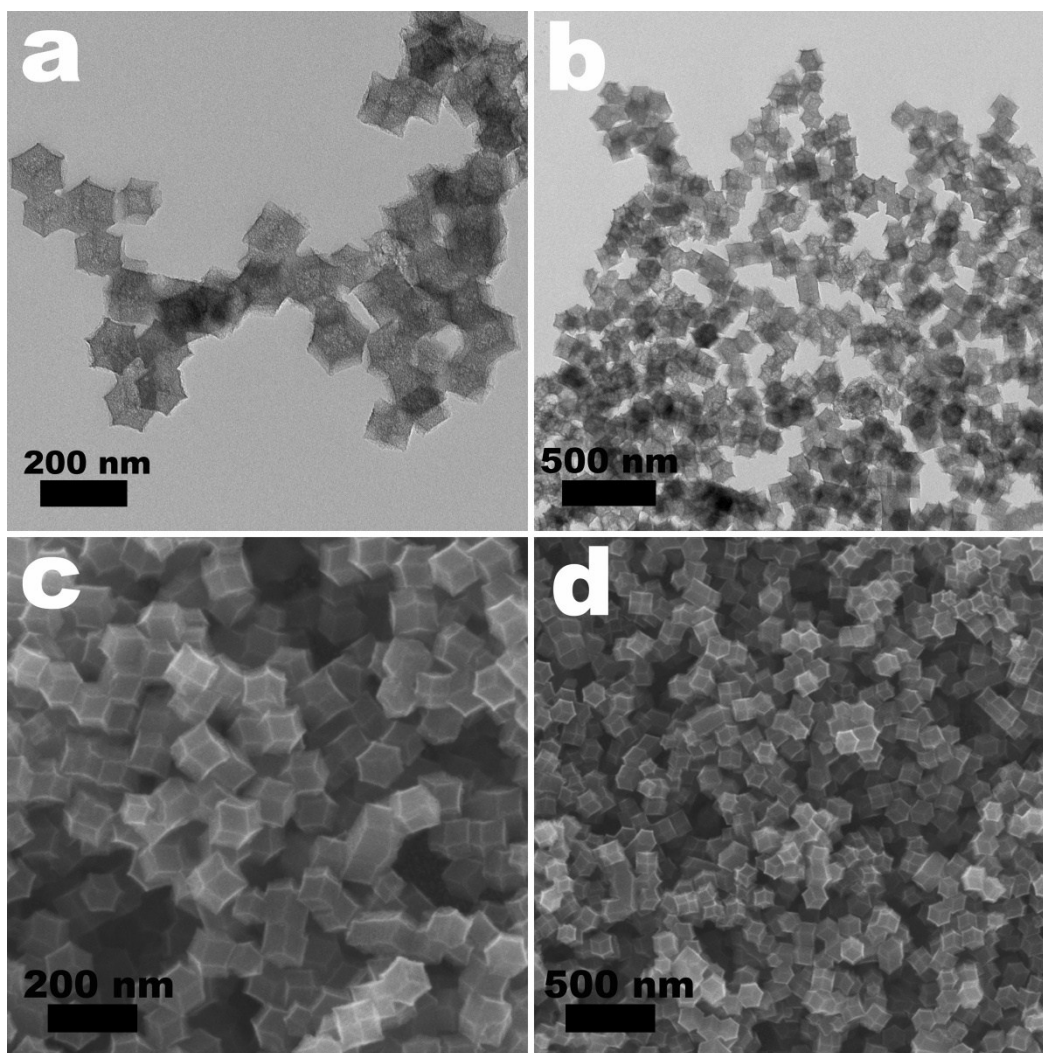
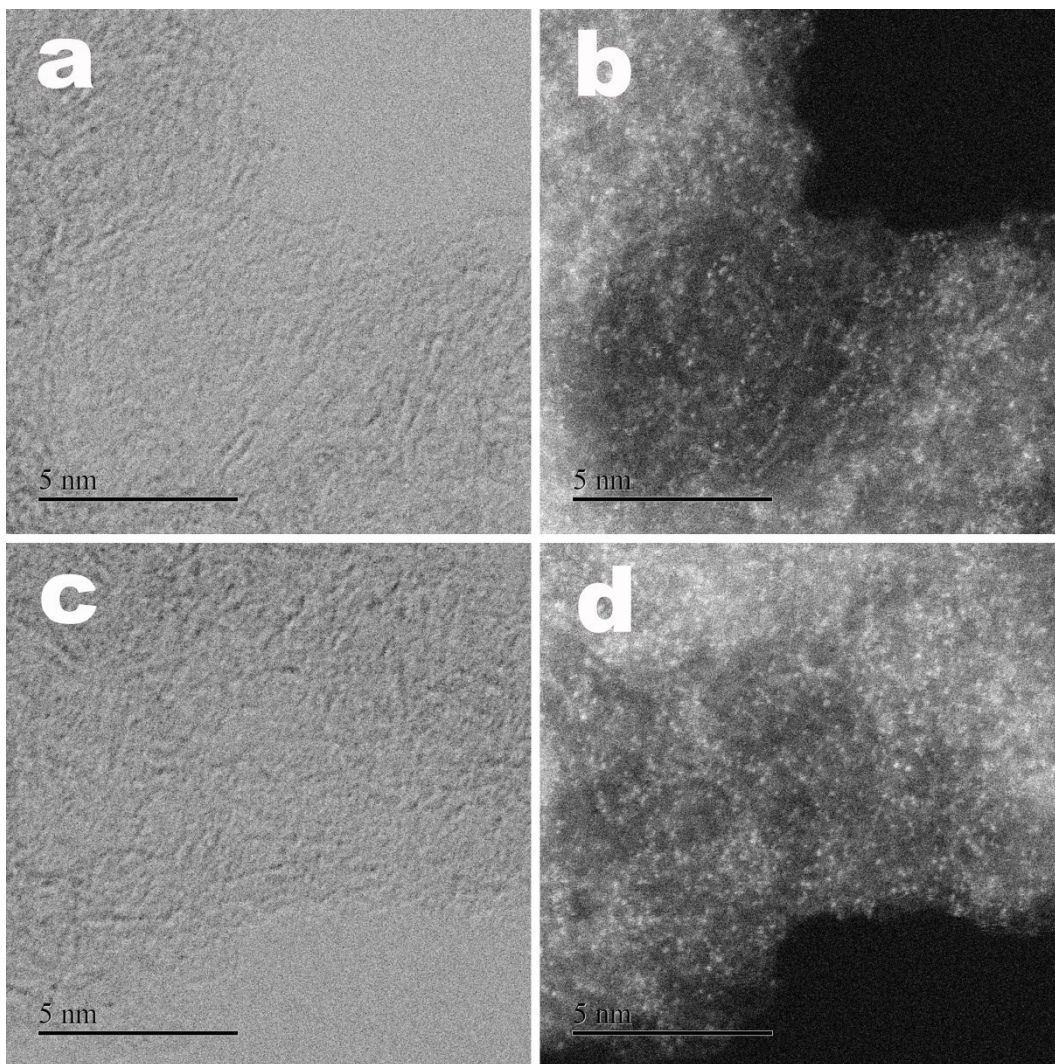


Figure S2. XRD patterns of the ZIF-8.



**Figure S3.** TEM image and SEM image of Fe SAEs.



**Figure S4.** Aberration corrected BF-STEM and HAADF-STEM images of Fe SAEs.

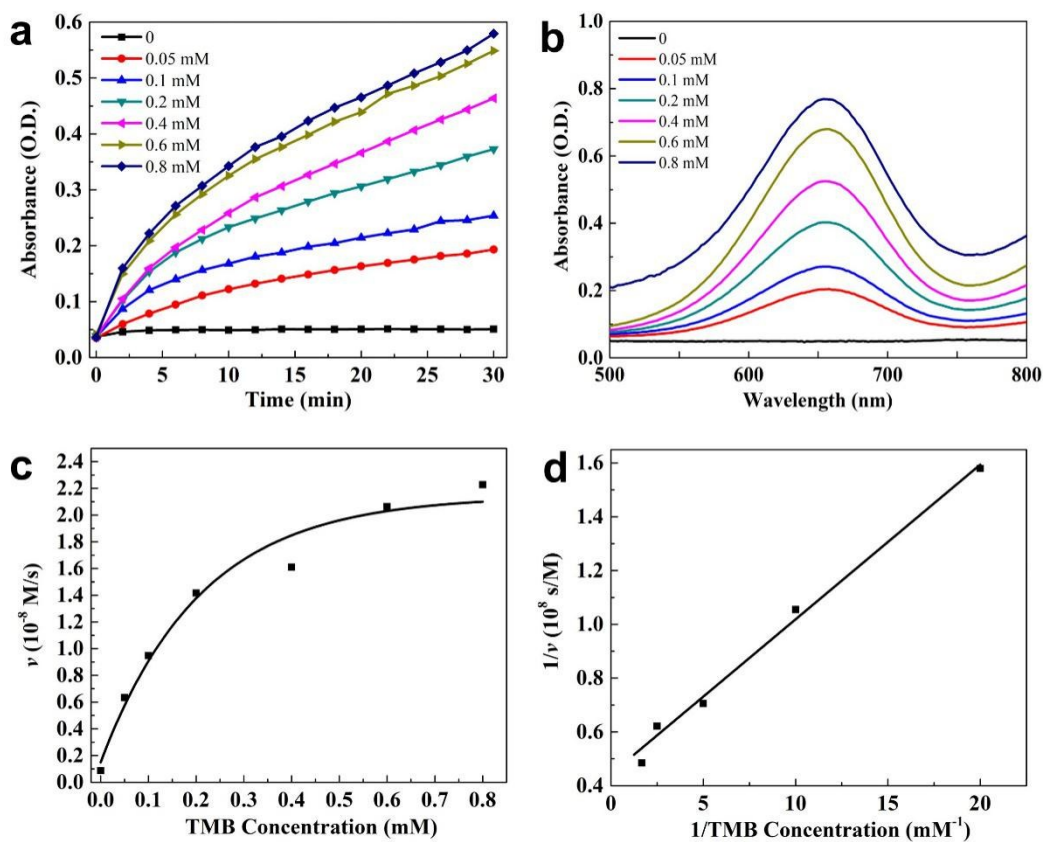


**Figure S5.** Oxidase-like catalysis of Fe SAEs to different concentration of TMB in the absence of  $\text{H}_2\text{O}_2$ . (a) Time course of catalysis. (b) The UV-Vis absorption spectra of the reactions with different TMB concentrations. (c) Michaelis-Menten kinetics for the oxidation of TMB catalyzed by Fe SAEs. (d) Lineweaver-Burk plot.

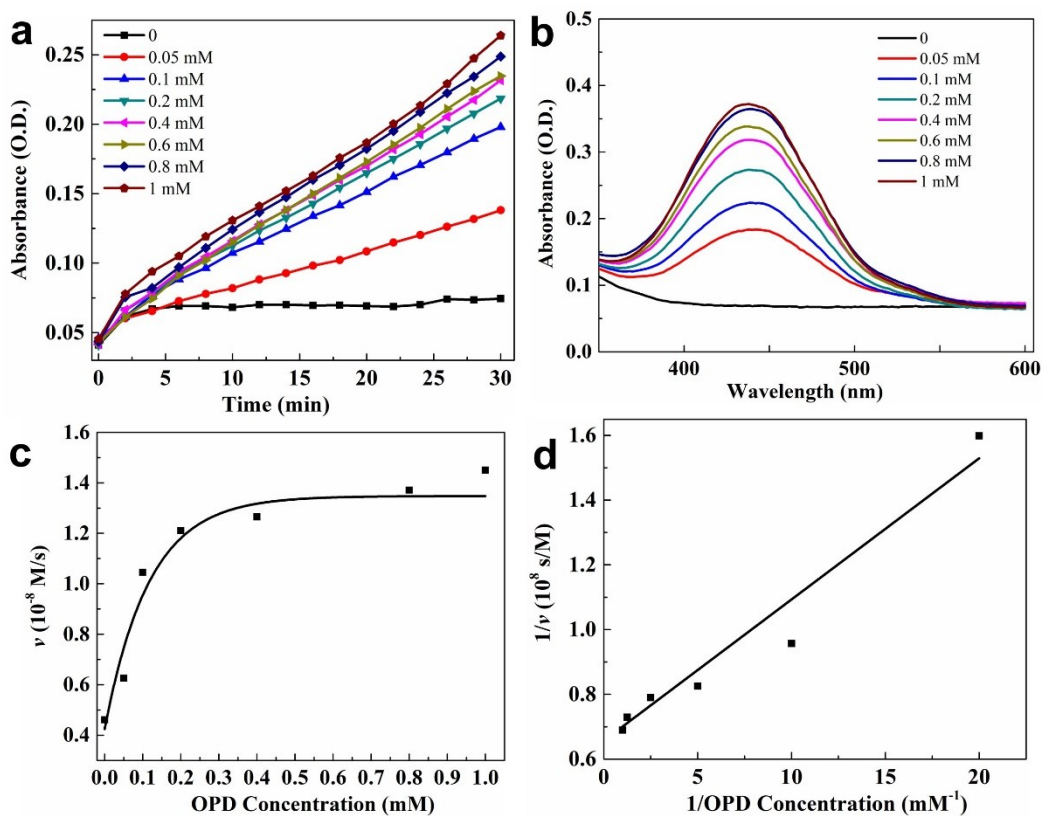


**Figure S6.** Oxidase-like catalysis of Fe SAEs to different concentration of OPD in the absence of  $H_2O_2$ . (a) Time course of catalysis. (b) The UV-Vis absorption spectra of the reactions with different OPD concentrations. (c) Michaelis-Menten kinetics for the oxidation of OPD catalyzed by Fe SAEs. (d) Lineweaver-Burk plot.

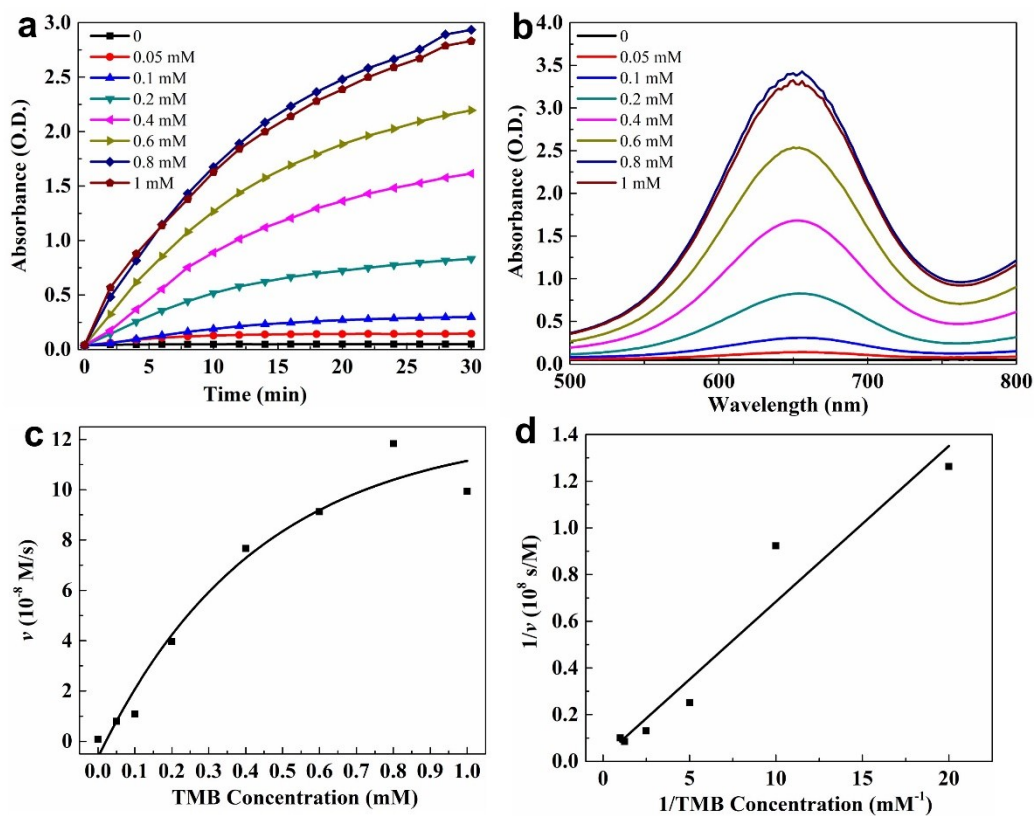


**Figure S7.** Peroxidase-like catalysis of Fe SAEs to different concentration of TMB at fixed concentration of  $\text{H}_2\text{O}_2$  (3mM). (a) Time course of catalysis. (b) The UV-Vis absorption spectra of the reactions with different TMB concentrations. (c) Michaelis-Menten kinetics for the oxidation of TMB catalyzed by Fe SAEs. (d) Lineweaver-Burk plot.

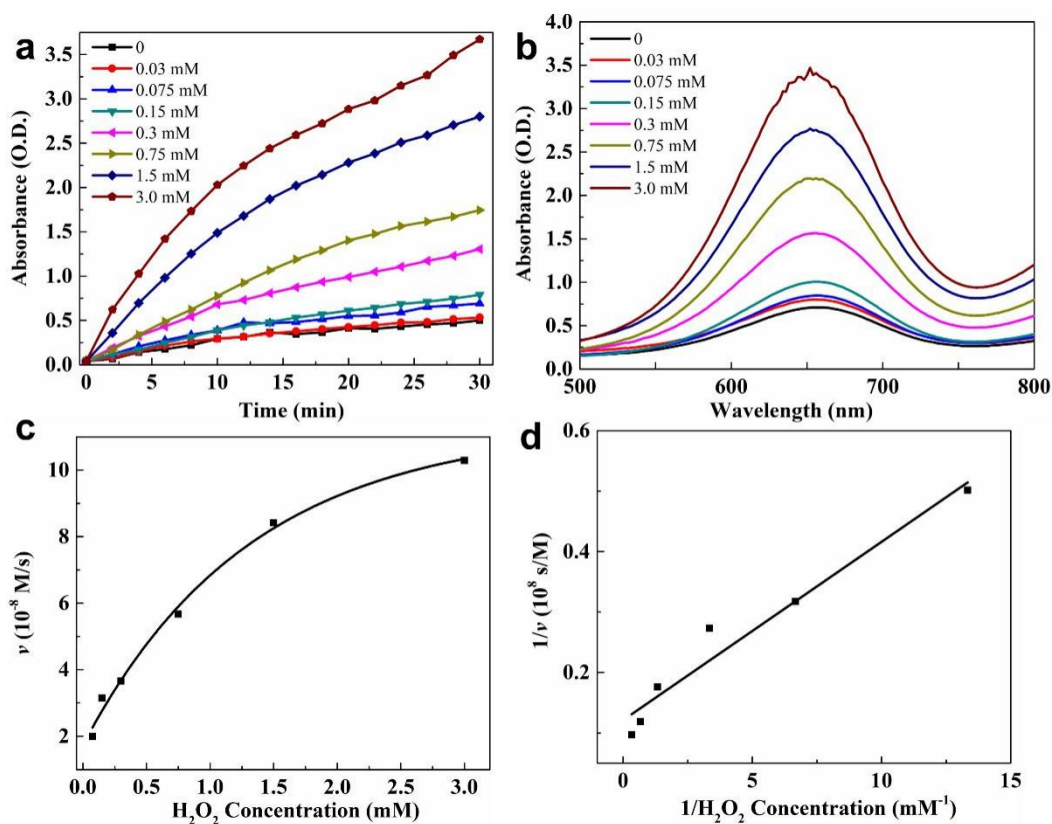


**Figure S8.** Peroxidase-like catalysis of Fe SAEs to different concentration of H<sub>2</sub>O<sub>2</sub> at fixed concentration of TMB (1mM). (a) Time course of catalysis. (b) The UV-Vis absorption spectra of the reactions with different H<sub>2</sub>O<sub>2</sub> concentrations. (c) Michaelis-Menten kinetics for the oxidation of H<sub>2</sub>O<sub>2</sub> catalyzed by Fe SAEs. (d) Lineweaver-Burk plot.

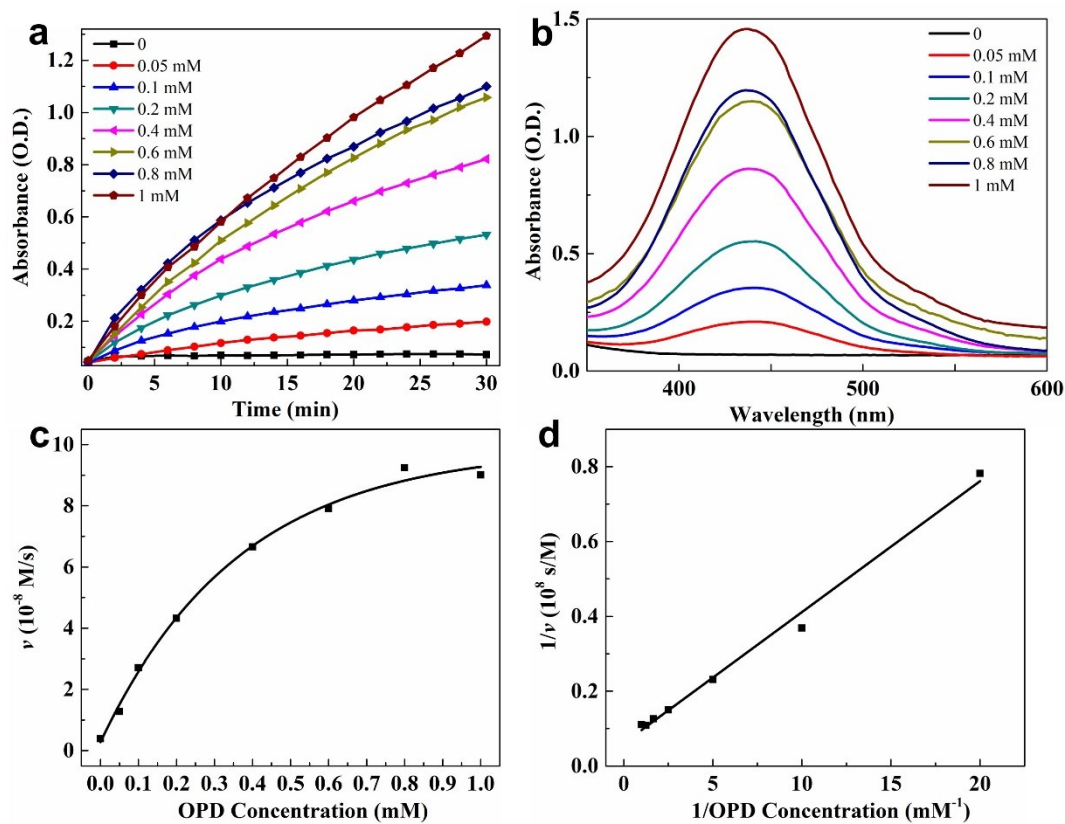


**Figure S9.** Peroxidase-like catalysis of Fe SAEs to different concentration of OPD at fixed concentration of  $H_2O_2$  (3mM). (a) Time course of catalysis. (b) The UV-Vis absorption spectra of the reactions with different OPD concentrations. (c) Michaelis-Menten kinetics for the oxidation of OPD catalyzed by Fe SAEs. (d) Lineweaver-Burk plot.

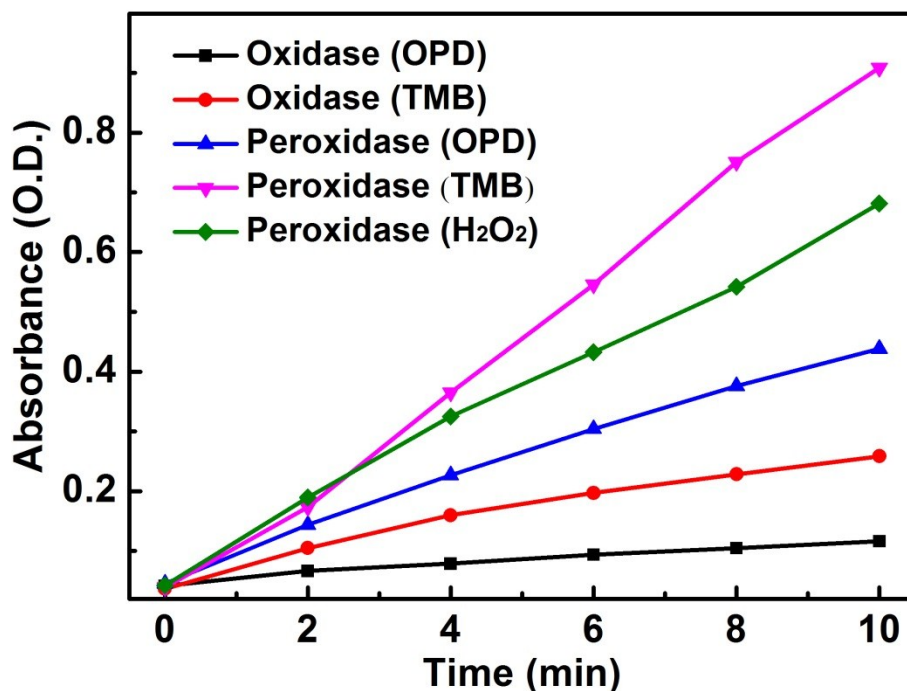


**Figure S10.** Oxidase and Peroxidase-like catalysis of Fe SAEs at the concentration of TMB (0.4mM), OPD (0.4mM) and H<sub>2</sub>O<sub>2</sub> (0.3mM).

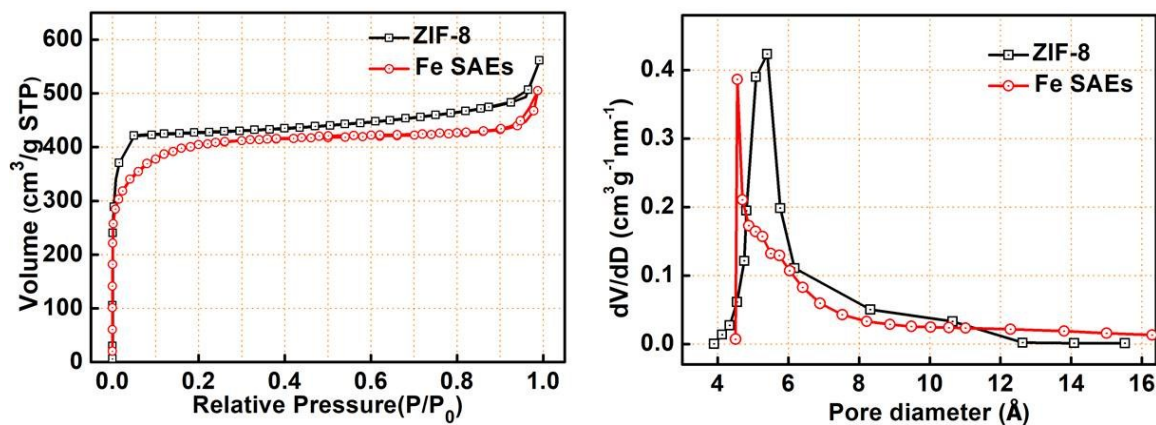


**Figure S11.** N<sub>2</sub> adsorption and desorption isotherms and pore diameter distribution of ZIF-8 and Fe SAEs.

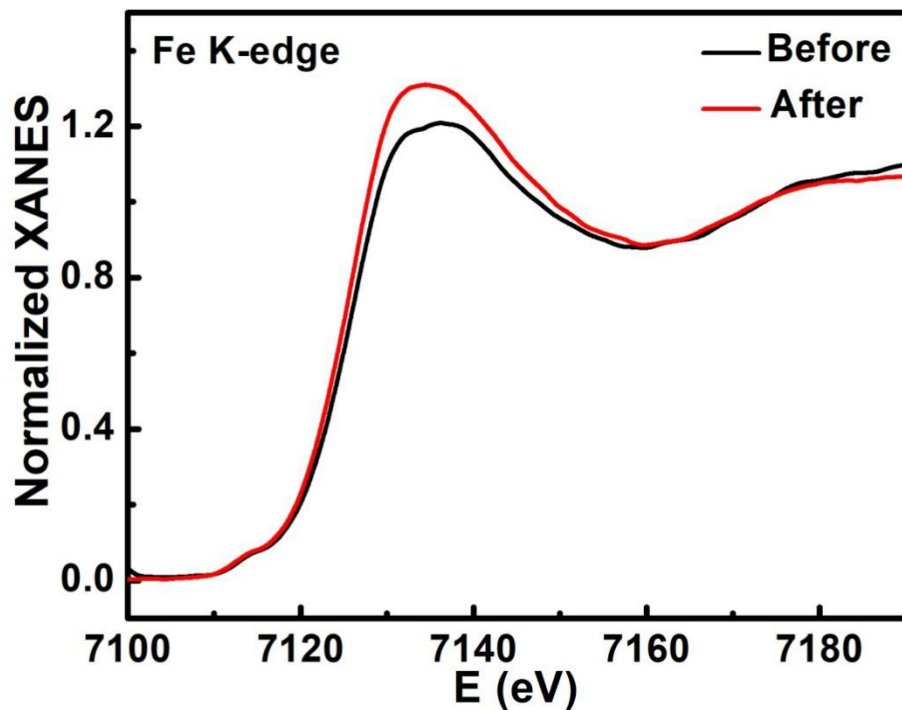


**Figure S12.** Comparison of white-line peak of Fe SAEs before and after reaction at *operando* XAFS measurements.

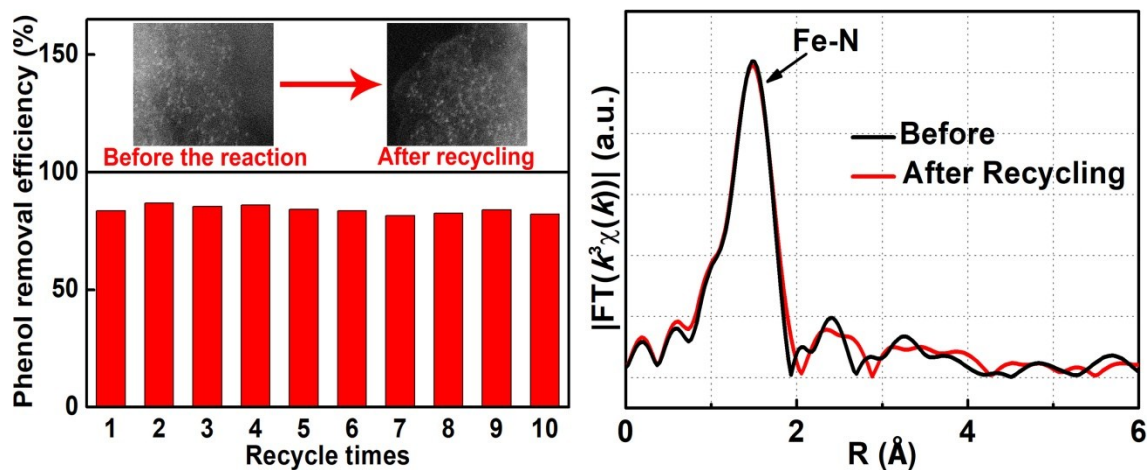


**Figure S13.** Reusability of the Fe SAEs in phenol degradation and the  $k^3$ -weighted  $\chi(k)$ -function of the EXAFS spectra at the Fe K-edge of Fe SAEs before and after recycling.

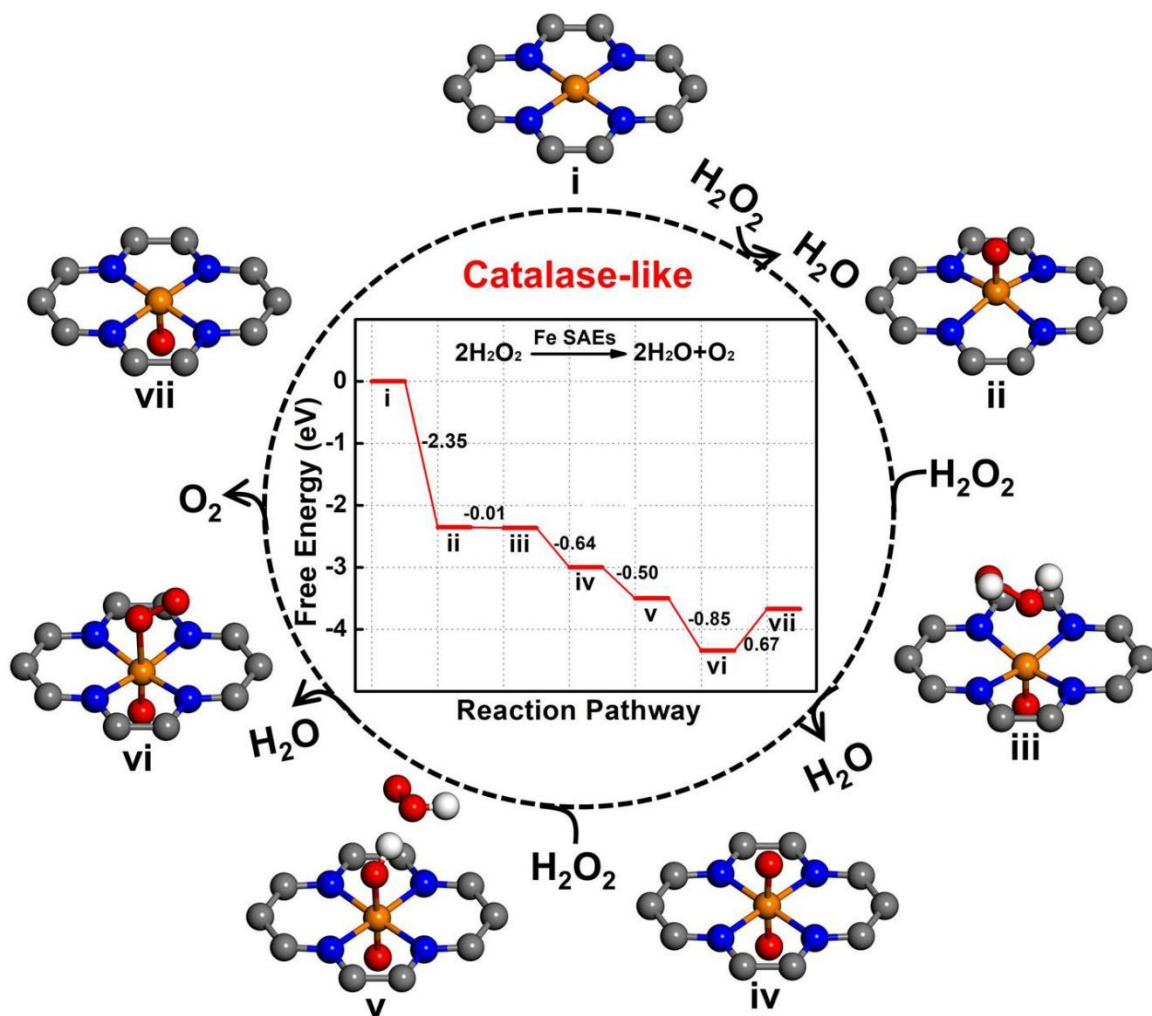


**Figure S14.** The optimized structures and transition state for catalase of Fe SAEs.

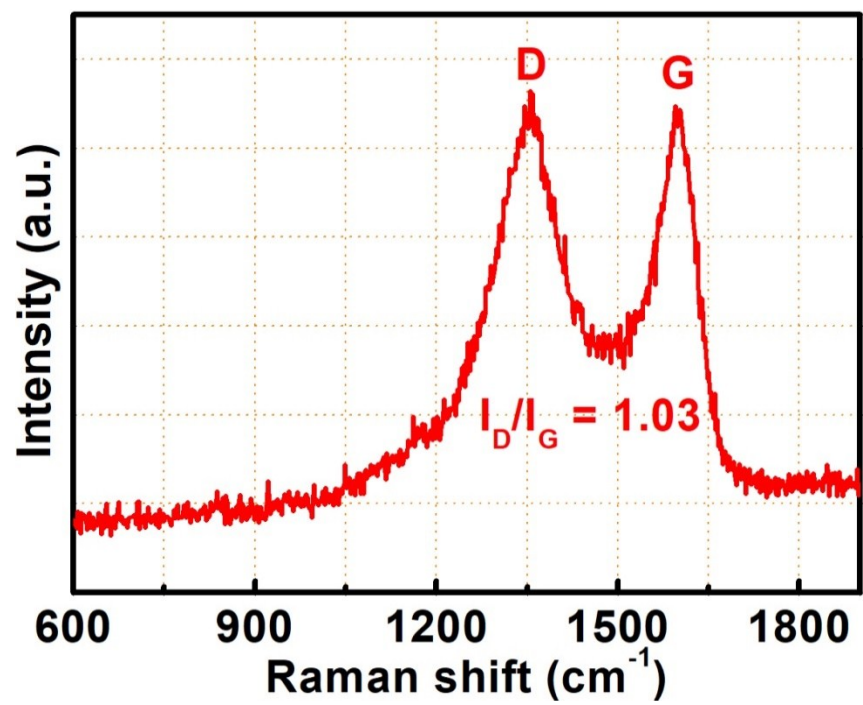


Figure S15. Raman spectrogram of the Fe SAEs.

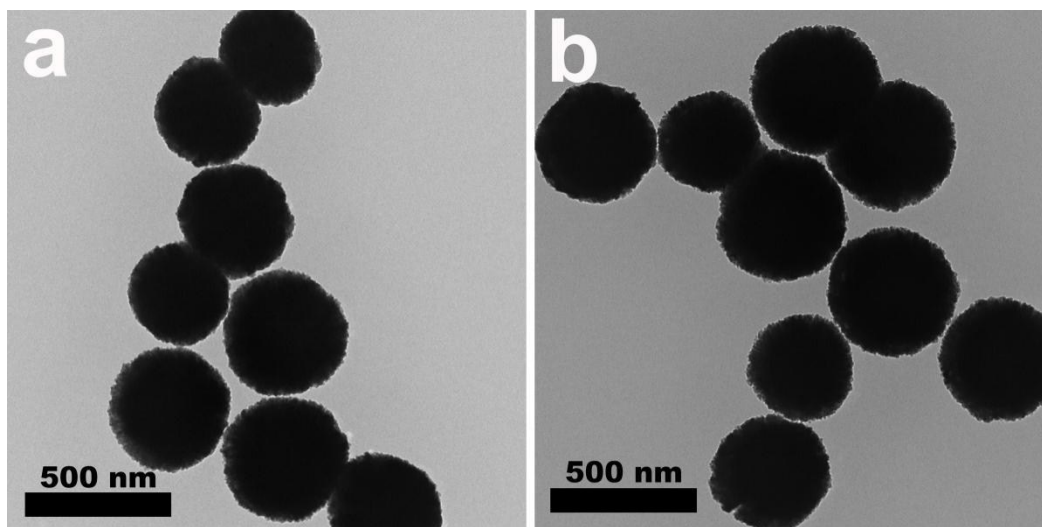


Figure S16. TEM images of Fe<sub>3</sub>O<sub>4</sub>.

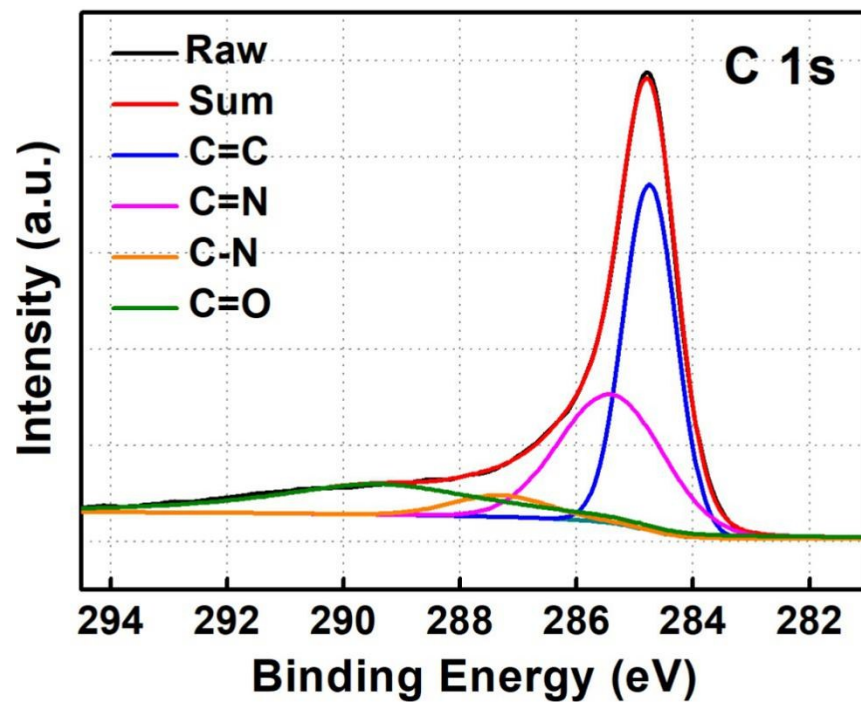


Figure S17. C 1s spectra of the Fe SAEs.

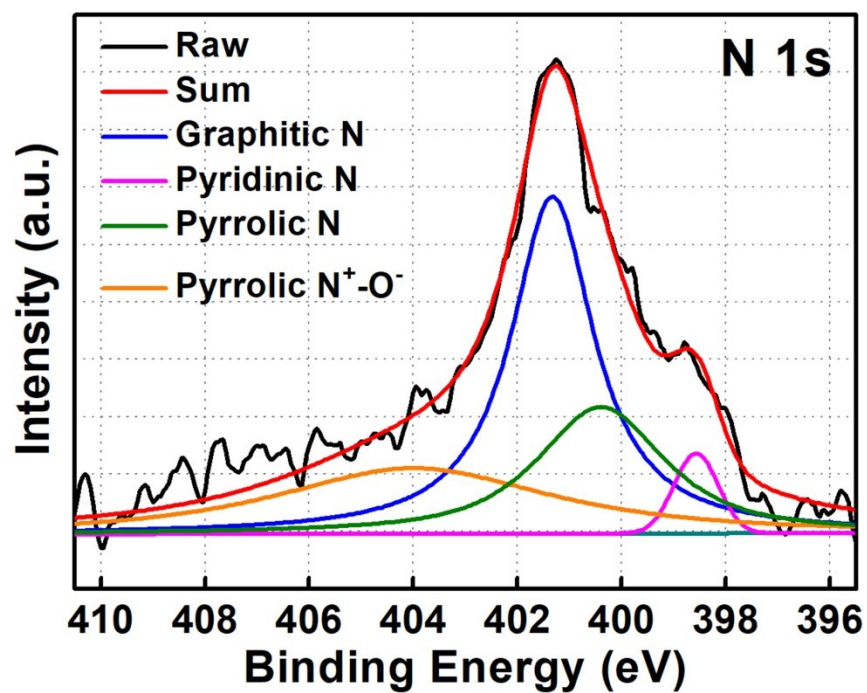


Figure S18. N 1s spectrum of the Fe SAEs.

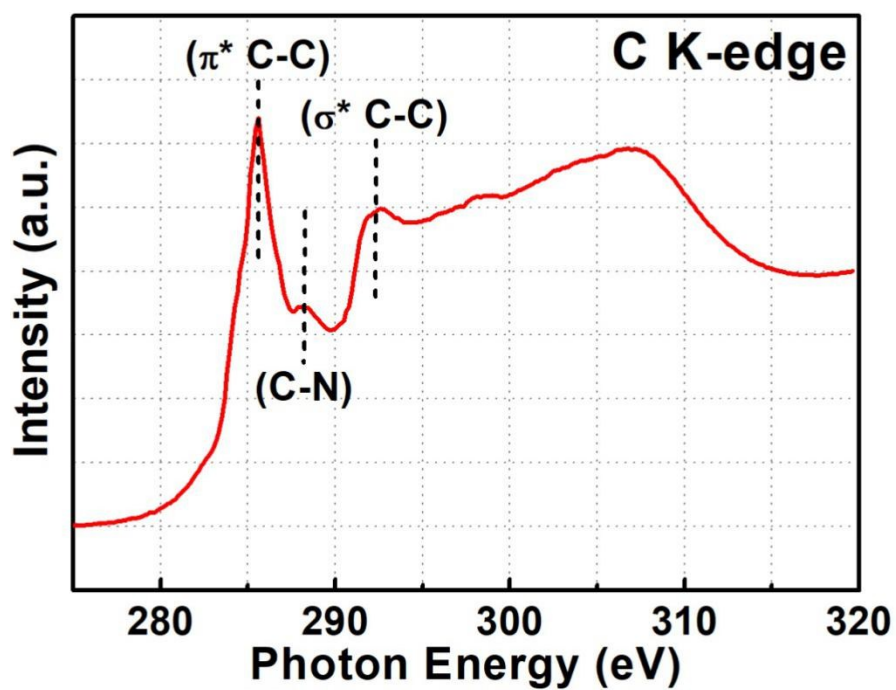


Figure S19. C K-edge of the Fe SAEs.

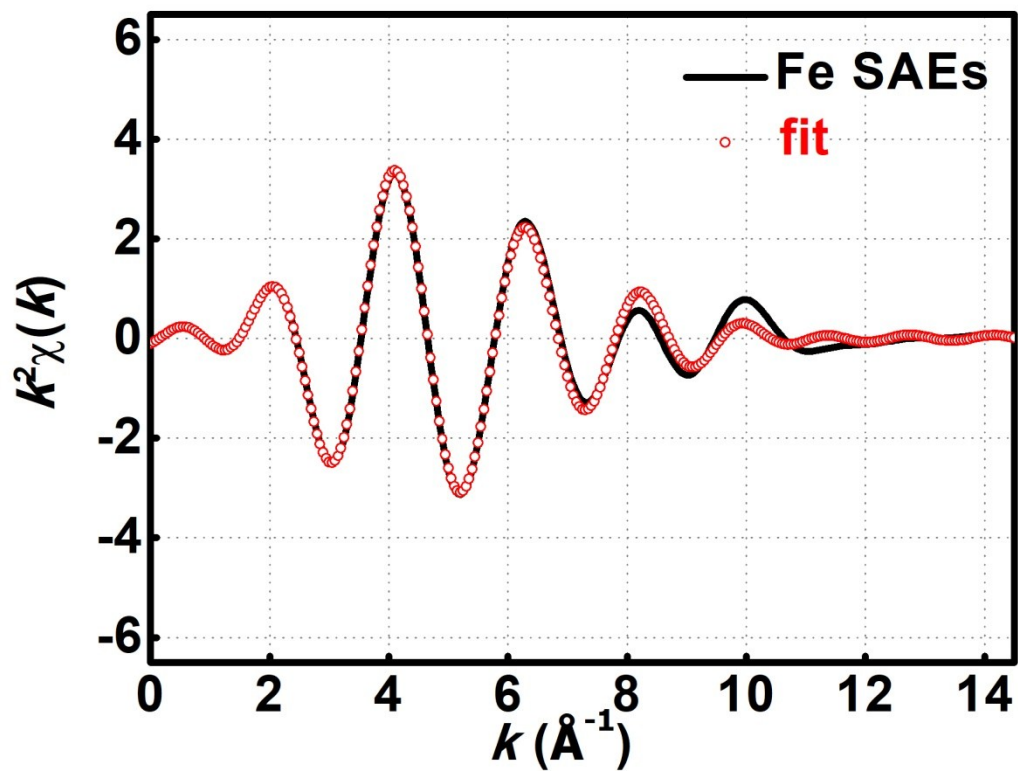


Figure S20. FT-EXAFS Fitting result of Fe SAEs.

**Table S1:** EXAFS data fitting results of Fe SAEs. ( $S_0^2=0.9$ )

Sample	Scatteringpair	CN	R(Å)	$\sigma^2(10^{-3} \text{ \AA}^2)$	$\Delta E_0(\text{eV})$	R-factor
Fe SAEs	Fe-N	4	2.04	2.1	-2.3	0.0002

CN, coordination number; R, interatomic distance;  $\sigma^2$ , Debye–Waller factor;  $\Delta E_0$ , edge-energy shift.

**Table S2:** The kinetic parameters of Fe SAEs.

Sample	Enzyme type	[E]M	Substrate	Km(mM)	Vmax(M/s)
Fe SAEs	Oxidase	$1.07 \times 10^{-6}$	TMB	0.13	$2.25 \times 10^{-8}$
Fe SAEs	Oxidase	$1.07 \times 10^{-6}$	OPD	0.066	$1.52 \times 10^{-8}$
Fe SAEs	Peroxidase	$1.07 \times 10^{-6}$	TMB	3.92	$5.88 \times 10^{-7}$
Fe SAEs	Peroxidase	$1.07 \times 10^{-6}$	H <sub>2</sub> O <sub>2</sub>	0.243	$8.25 \times 10^{-8}$
Fe SAEs	Peroxidase	$1.07 \times 10^{-6}$	OPD	0.572	$1.63 \times 10^{-7}$